JOURNAL OF CATALYSIS **169,** 67–75 (1997)
ARTICLE NO. CA971698

Alcohol Dehydration Reactions over Tungstated Zirconia Catalysts

Gustavo Larsen,[1] Edgar Lotero, Lucía M. Petkovic, and David S. Shobe

Department of Chemical Engineering, University of Nebraska, Lincoln, Nebraska 68588-0126

Received November 26, 1996; revised March 13, 1997; accepted March 14, 1997

The behavior of tungstated zirconia (WZ) toward dehydration of 1-propanol, 2-propanol, and *tert*.-butanol was compared with that of H-mordenite. For 1- and 2-propanol, the desorption temperatures of olefinic products formed over the WZ catalyst were found to be very close to those observed in H-mordenite; however, the zeolite catalyst had a much larger tendency to retain (or to readsorb) olefins in the pores in the form of oligomerization products, as evidenced by the detection of the $m/e = 65$ signal (cyclopentadienyl cation) during the temperature-programmed reaction of 2-propanol. The Brønsted acid sites of the zeolite underwent rapid H^+/D^+ exchange when 2-propanol deuterated in its hydroxyl group was used. This allowed the olefinic products to incorporate deuterium during reaction. On the other hand, the WZ catalyst did not effect the H^+/D^+ exchange of propene formed from CH_3–HCOD–CH_3, presumably because olefin readsorption onto hydrated W^{6+} sites does not take place. The structure of the WZ catalyst was monitored by EXAFS and XRD.

1. INTRODUCTION

Tungstated zirconia (WZ) is a strong solid acid (1–7), and has been proposed as a good candidate for the isomerization of alkanes heavier than C_4. Using the isomerization of *n*-butane over platinum supported on WZ (PtWZ) in the presence of hydrogen as the test reaction, we were recently able to study the effect of preparation variables such as metal loading and calcination and reduction temperatures (7). A unique aspect of WZ and PtWZ is that W–O–W bonds may be present in WZ catalysts active for alkane isomerization (2). This does not occur in sulfated zirconia, where the active site is believed to be isolated sulfate moieties. By means of Raman spectroscopy, Wachs *et al.* (8) found that W–O–W bonds are formed in WZ prepared from aqueous impregnation even after calcination temperatures as low as 773 K and W loadings in the 3–5 wt% range.

In previous work, we used IR spectroscopy of adsorbed pyridine to study the acidity of our WZ preparations (3, 4), but we still felt that a better acidity scale is generally obtained by carrying out reaction experiments. Thus, the "catalytic" acidity of tungstated zirconia samples was monitored by temperature-programmed alcohol dehydration reactions and compared with that of H-mordenite. The zeolite reference catalyst was chosen based on our previous observation that it displays *n*-butane isomerization activities comparable to that of WZ. In this paper, we wanted to check whether such similarities could be extended to other fundamentally different acid-catalyzed reactions such as alcohol dehydrations. X-ray diffraction (XRD), X-ray absorption spectroscopy (XAS), and nitrogen physisorption were used to study the structural properties of WZ.

[1] To whom all correspondence should be addressed. Fax: 402-472-6989. E-mail: glarsen@unlinfo.unl.edu.

2. EXPERIMENTAL

a. Catalyst Preparation

The preparation of WZ (W content: 6 wt%) is described elsewhere (4). In brief, the catalyst is obtained by aqueous incipient wetness impregnation of hydrous zirconia with a solution containing the appropriate amount of ammonium metatungstate. The sample is subsequently calcined at 1096 K for 1 h under flowing air. The surface area of the tungstate-free support was 3 m^2/g, while that of WZ was 36 m^2/g. The H-mordenite reference catalyst was kindly donated by Dr. Alan Risch from UOP, Tarrytown, New York. It has a Si/Al ratio of 6.4. The hydrogen form of the zeolite was obtained *in situ* prior to the temperature-programmed experiments by thermal decomposition of the ammonium form at 893 K.

b. X-Ray Absorption Measurements

The XAS experiments at the L_{III} edge of W were performed using synchrotron radiation at beamline X-18b of the National Synchrotron Light Source, Upton, New York. The WZ sample was pressed into a disk after diluting it with an appropriate amount of low-surface-area Al_2O_3 (2 m^2/g) to get adequate X-ray background absorption (unlike Al_2O_3, the zirconia support is a strong background absorber). Data analysis was performed using the single-scattering formalism, using the program FEFFIT from the UWXAFS set of programs (10). The use of multiple scattering was not justified because the latter requires a priori the proposal of a model structure (or very few model

0021-9517/97 $25.00

structures) to fit the spectra. Such approach is most adequate for "ideal" structures, such as framework transition metal ions in zeolites, but would not be realistic for a catalyst with pronounced site heterogeneity. The WZ sample was precalcined at 1096 K in our laboratory, and dried *in situ* under nitrogen for 1 h at 773 K prior to reduction under 5% H_2/N_2 flow at 623 K. The reduction process has shown to have no influence on the XRD patterns and decreases the intensity of the W L_{III} white line only by about 5–10%, even when 1 wt% Pt is added to the system (3), indicating that the XAS spectrum is dominated largely by W^{6+} species. Previous TPR results are also consistent with this picture (3). We were able to measure the oxygen backscattering around W in WZ (containing 1 wt% Pt).

c. X-Ray Diffraction and Adsorption Measurements

The XRD patterns of calcined WZ and Z (W-free support) samples were recorded on a Rigaku DMAX/IIB diffractometer (with Cu $K\alpha$ radiation of 1.5418 Å). Surface areas were evaluated by the BET method using a conventional glass line capable of absolute pressures around 10^{-6} Torr, equipped with grease-free stopcocks and a digital pressure transducer.

d. Temperature-Programmed Reaction (TPReac) of tert.-Butanol, 1-Propanol and 2-Propanol

The WZ sample (150-mg catalyst bed) was calcined *in situ* at 1096 K prior to cooling the TPReac quartz cell to room temperature. The air flow was switched to pure helium and the cell purged for about 15 min prior to injection of 10 μl alcohol at the reactor inlet. An MKS residual gas analyzer was used to follow a total of 16 different *m/e* ratios. In the figures, all masses are plotted with no attenuation factors involved unless specified otherwise in the figure legends. After injection of the alcohol the cell was purged for another 15 min to remove most of the reversibly adsorbed alcohol prior to ramping the temperature at a 3.1 K/min rate under mass-flow controlled He. The H-mordenite reference sample was calcined at 873 K prior to TPReac experiments.

3. RESULTS AND DISCUSSION

We used XRD and EXAFS to gain some insight into the W^{6+} structure. The XRD analysis shows that a larger extent of stabilization of the tetragonal ZrO_2 phase is achieved when tungsten is present (Fig. 1), this being the only difference between the two patterns. Some minor peaks detected previously (e.g., around 23° and 38°) were originally attributed to a separate WO_3 (4). These were not observed in our new preparations. The latter could have been due to the presence of an impurity in the XRD specimen. We take the disappearance of the strong reflections at $2\theta \sim 30.5$ and 51 as indicative of degradation of the tetragonal structure. On the other hand, the two peaks vicinal to the strongest signal in the WZ XRD pattern (Fig. 1, $2\theta \sim 30.5$) are due to the presence of monoclinic zirconia. Figures 2a–c show the k^1-weighted EXAFS, the isolated first-shell EXAFS function, and the Fourier transform magnitude, respectively. The first-shell coordination distance (R_{W-O}) and coordination number (N_{W-O}) were found to be 1.69 and 4.7 respectively. Given the 15–20% error in EXAFS-derived coordination numbers, we can only infer that there are unsaturated W centers at the surface. Previous XANES data indicated that a distorted octahedral symmetry is the most plausible geometry of the tungsten moieties (3). Unfortunately, the quality of the data at k values higher than 12 $Å^{-1}$ did not allow us to model metal–metal (second-shell) backscattering in a reliable way; however, since there is Raman evidence (8) for the formation of W–O–W bonds on the surface of tungstated zirconia at both lower calcination temperatures and W loadings lower than those employed in this work, we are inclined to believe that the lack of a W EXAFS second-shell detection does not necessarily imply the presence of isolated W centers in our catalysts. We had to use such high calcination temperatures because this was a requirement to achieve optimum *n*-butane isomerization activities (4, 7).

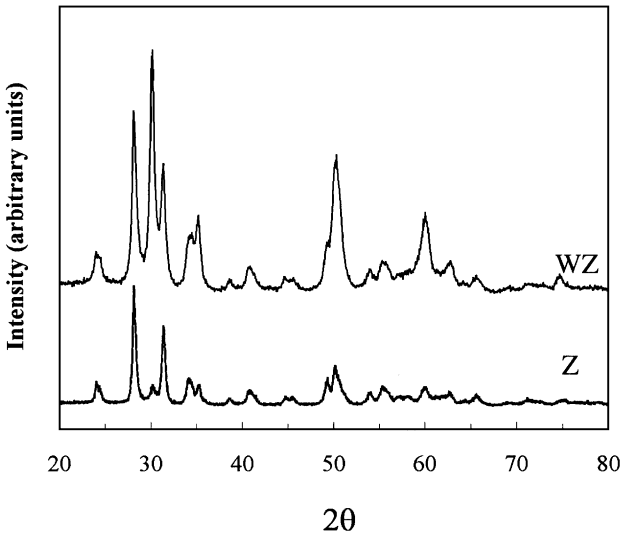

FIG. 1. XRD patterns of WZ and Z samples.

The use of TPReac of alcohols for probing acidity has been proposed in the past (11). The central idea is that alcohols with different degrees of substitution should in principle display different reactivities for olefin formation. This is because during TPReac, the hydrogen-bonded alcohol is expected to undergo dehydration (to either ethers or olefins) or desorption with no reaction. The TPReac of 2-propanol often shows evidence for acetone formation via dehydrogenation of the alcohol on basic sites (12, 13). With the exception of those cases in which dehydration to olefins

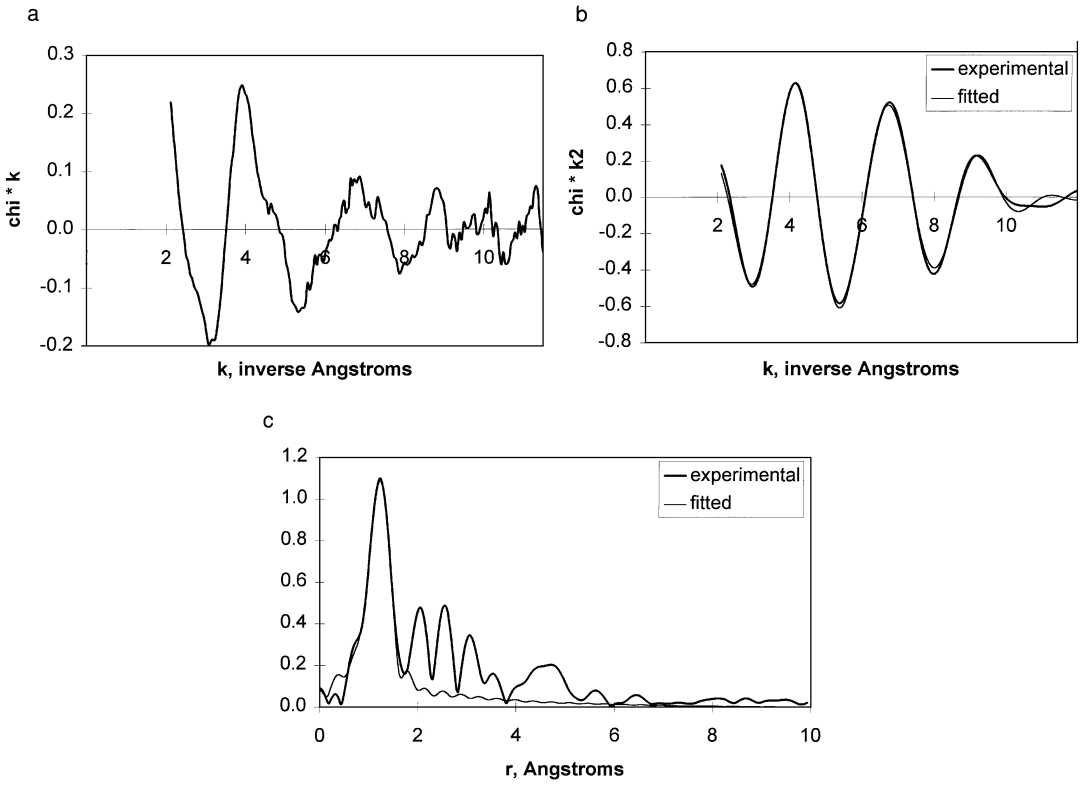

FIG. 2. W L_{III} EXAFS on WZ. (a) k^1-EXAFS function, (b) isolated first-shell EXAFS and fit, and (c) FFT magnitude and fit.

is fairly restricted [e.g., TPReac of adsorbed methanol (5)], formation of ethers requires high acid site density and low acid strength (14). Thus, the ability of a strong solid acid to retain the alcohol molecule on the surface to the point in temperature at which it yields olefinic products can be taken as a measure of its acid strength. A priori, we expect t-butanol to undergo facile dehydration at low temperatures because an adsorbed species with strong tertiary carbenium ion character is most likely to form on the surface. On the other hand, less substituted alcohols such as 1-propanol are expected to be less reactive. Alcohol dehydrations are expected to be better acidity probes than alkane isomerizations for oxoanion-loaded zirconias because it is now believed that other factors affect reactions with alkanes (15). For example, Sachtler and co-workers (15) showed that while dramatic *n*-butane isomerization activity differences between sulfated zirconia and sulfated zirconia promoted with iron and manganese are found, these two materials display very similar acidity levels in light of spectroscopic data. In addition, it would be fundamentally interesting to use a good chemical probe to compare a solid protonic acid such as H-mordenite with Lewis solid acids such as high-temperature calcined tungstated zirconias.

The TPReac curves for t-butanol over WZ are shown in Fig. 3. As mentioned above, a total of 16 masses including those relevant to ether formation and t-butanol desorption were followed. Here, we show only those signals detected

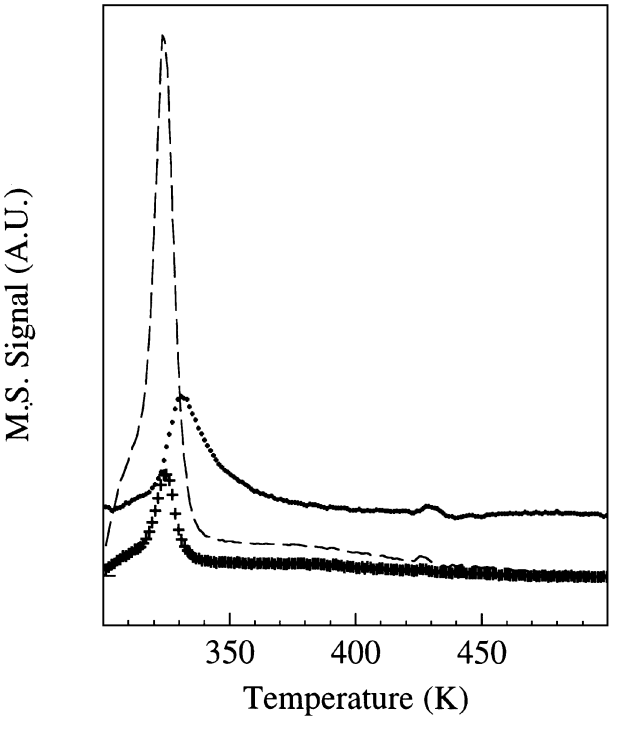

FIG. 3. TPReac of t-butanol over WZ. $m/e = 18$ (dotted), 41 (dashed), and 55 (+).

that are representative of a particular chemical species. For example, $m/e = 41$ (allyl cation) is indicative of olefin formation. No t-butanol was found to leave the catalyst surface ($m/e = 59$). Figure 3 shows that isobutene starts forming immediately after the beginning of the TPReac experiment. As expected from the isobutene fragmentation pattern, the $m/e = 55$ signal in Fig. 3 is relatively small and follows a trend similar to that of the $m/e = 41$ peak; however, for heavier alkenes such as octenes, the $m/e = 55$ becomes dominant (16, 17). The m/e 41 to m/e 55 ratio is consistent with formation of isobutene, suggesting that the C_4 olefin is desorbed prior to oligomerization. It is clear that WZ is characterized by a quick release of the isobutene product around 320–325 K. Interestingly, we found that coke deposition is negligible in WZ samples, as evidenced by temperature-programmed oxidation of spent samples. This did not surprise us since we had found that very small amounts of coke are deposited after the isomerization of *n*-butane over WZ samples (4). Iglesia *et al.* (2) suggested that the surface residence time of carbocationic intermediates produced during the isomerization of *n*-heptane over PtWZ is much smaller than that in $PtSO_4$=Z. This conclusion was reached based on the weak dependence of the isomerization rates with the addition of good hydride transfer agents such as adamantane and the negative hydrogen order dependence of the isomerization pathway (3).

Also as a reference, the same experiment with t-butanol was carried out using the W-free support (Fig. 4). The intensities of the three strongest signals (m/e 18, 41, and 55) were roughly two orders of magnitude smaller than those observed in WZ; however, a shift of the olefin peak of about 35–40 K indicates the lower acid strength of the tungsten-free support with respect to WZ. Furthermore, even when normalized to surface area, the MS signals from TPReac of *tert*.-butanol on Z are about one order of magnitude lower than those of WZ. Thus, we decided to focus on WZ and H-mordenite instead because the zirconia support does not appear to play a major role in this reaction.

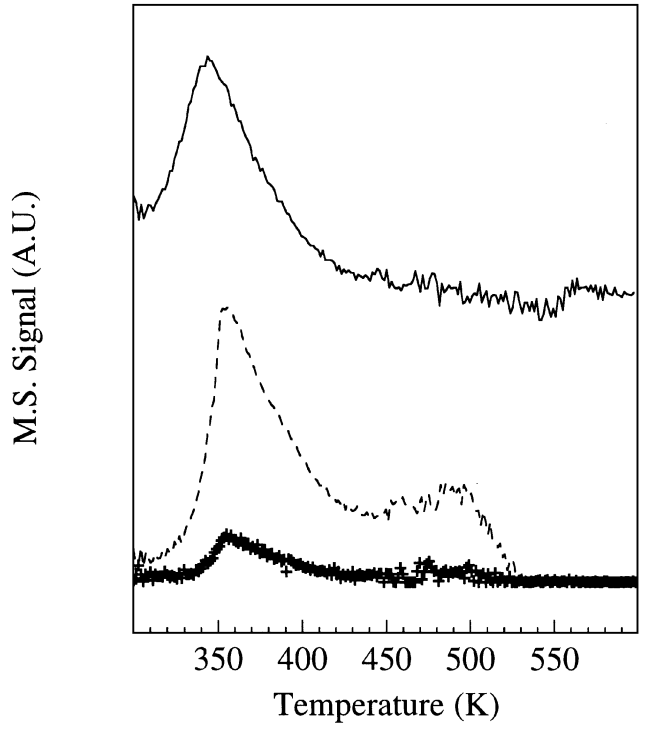

FIG. 4. TPReac of t-butanol over Z. $m/e = 18$ (solid), 41 (dashed), and 55 (+).

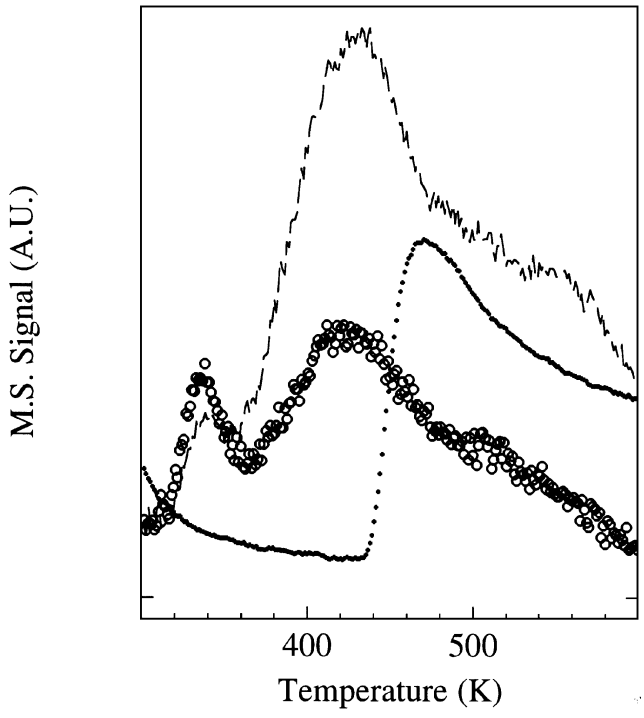

FIG. 5. TPReac of t-butanol over H-mordenite. $m/e = 41$ (dashed), 18 (dotted), and 57 (○).

The behavior of H-mordenite for t-butanol TPReac differs from that of WZ. A small contribution to $m/e = 41$ suggests the presence of olefins in the gas phase, while $m/e = 57$ is indicative of either di-t-butyl ether or t-butanol desorption (Fig. 5). The idea that heavy oligomers were trapped inside the zeolite pores was confirmed by a TPO experiment up to 1023 K. After quantification of the carbon residues by injection of known amounts of CO_2 at the inlet of the reactor following the reoxidation experiment, we found that 2.4% of the carbon from the 10-μl t-butanol pulse was left on the solid as residue. An interesting feature is that, unlike WZ, H-mordenite does not have the ability to release isobutene at low temperatures.

Figures 6 and 7 show that comparable amounts of reacted-to-unreacted 1-propanol are observed in both catalysts. The $m/e = 59$ signal ($C_3H_7O^+$) is generated by both alcohol and ether fragmentation, but a comparison with $m/e = 31$ (which is essentially due to the alcohol molecule)

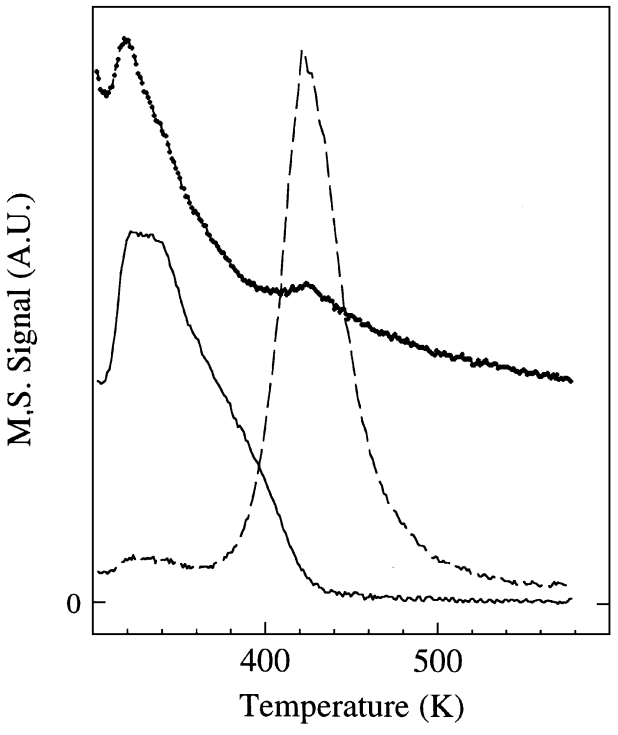

FIG. 6. TPReac of 1-propanol over WZ. $m/e = 41$ (dashed), 18 (dotted), and 31 (solid).

shows that a very small amount of ether is produced around 440 K over H-mordenite. No ether signals were detected during TPReac of 1-propanol over WZ. The olefin desorption temperatures are very similar in both catalysts, suggesting that these materials behave similarly in terms of acid strength.

In a previous study, we found that methanol desorbed from WZ during TPReac experiments in the form of dimethyl ether (DME) at temperatures slightly lower than those observed in H-Y zeolite and much lower than those of tungstated aluminas. However, the H-Y zeolite catalyst turned dark gray after the desorption experiment with methanol, whereas the WZ sample retained its pale yellow color (5). It appears that the acidity of WZ is comparable to that of zeolites, but an interesting feature of WZ is its very low tendency to catalyze the oligomerization of the alkene primary products. The ability of WZ to release olefins by dehydration without significant carbon deposition is consistent with the idea of a short-lived carbenium-like intermediate (2).

We have used 2-propanol, in the form of CH_3–HCOH–CH_3 and CH_3–HCOD–CH_3, in both catalysts in an attempt to understand in more detail the differences in the chemistry of alcohol dehydration between WZ and H-mordenite. In the case of unlabeled 2-propanol, the $m/e = 45$ is due to the presence of 2-propanol in the gas phase, whereas the $m/e = 58$ fragment is also due to acetone that might result from alcohol dehydrogenation over the catalyst basic sites (12, 13). Thus, to monitor the nonreactive alcohol desorption and acetone production with unlabeled 2-propanol, it is necessary to follow the $m/e = 45$ and 58 fragments simultaneously (16, 17). Figures 8 and 9 show that very small differences in the olefin desorption temperatures are observed in both catalysts when unlabeled 2-propanol is used (sharp low-temperature component in the case of H-mordenite, see Fig. 9). An interesting feature is that a small $m/e = 65$ peak (cyclopentadienyl fragment) was observed in the zeolite catalyst only at around 560 K. The cyclopentadienyl ion is indicative of catalyst coking. Thus, we propose, that the secondary alcohol yields both high-molecular-weight species ($m/e = 65$ and high-temperature $m/e = 41$ shoulders) and propylene (sharp $m/e = 41$ low-temperature peak) over H-mordenite. The $m/e = 58$ in H-mordenite (Fig. 9) is likely due to saturated alkyl chains since the hydrogen form of the zeolite is not expected to possess basic sites.

Using 2-propanol deuterated in its hydroxyl group caused the olefins in H-mordenite to rapidly incorporate deuterium in their hydrocarbon skeleton (Fig. 10). Interestingly, the $m/e = 41$ to 42 ratio is roughly 0.9 : 1 at the low-temperature desorption maximum (assigned to propylene). But the $m/e = 42$ signal (monodeuterated propenyl ion) became more important at higher temperatures. This suggests that readsorption of the olefinic products to yield deuterated alkenes (and oligomers, see $m/e = 65$ in Fig. 9) is

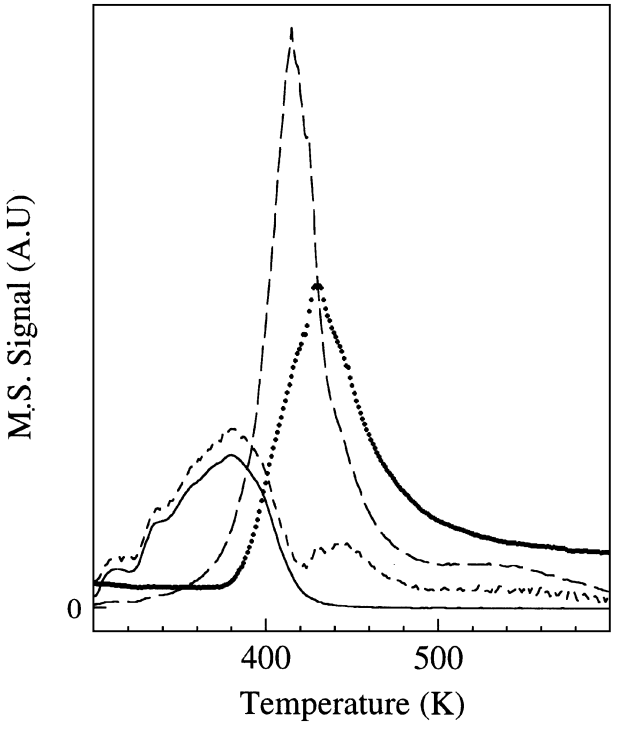

FIG. 7. TPReac of 1-propanol over H-mordenite. $m/e = 41$ (long-dashed), 18 (dotted), 59 (short-dashed), and 31 (solid).

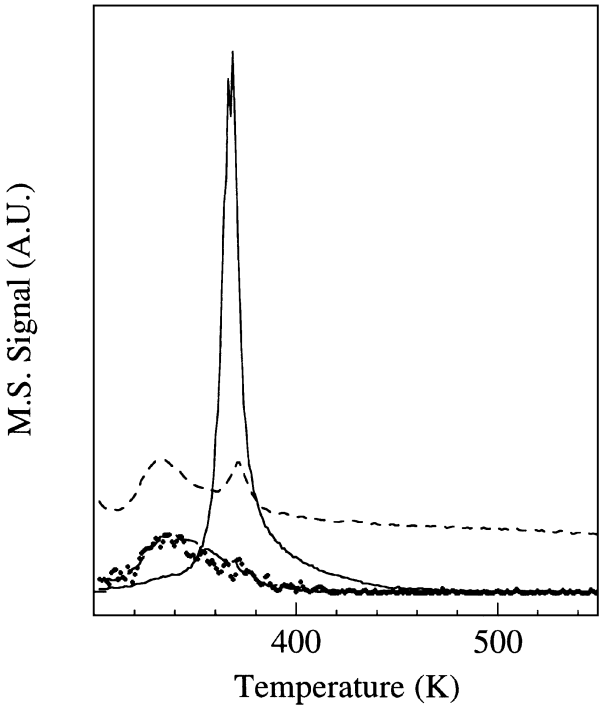

FIG. 8. TPReac of 2-propanol over WZ. $m/e = 41$ (solid), 18 (short-dashed), 45 (long-dashed), and 58 (×10, dotted).

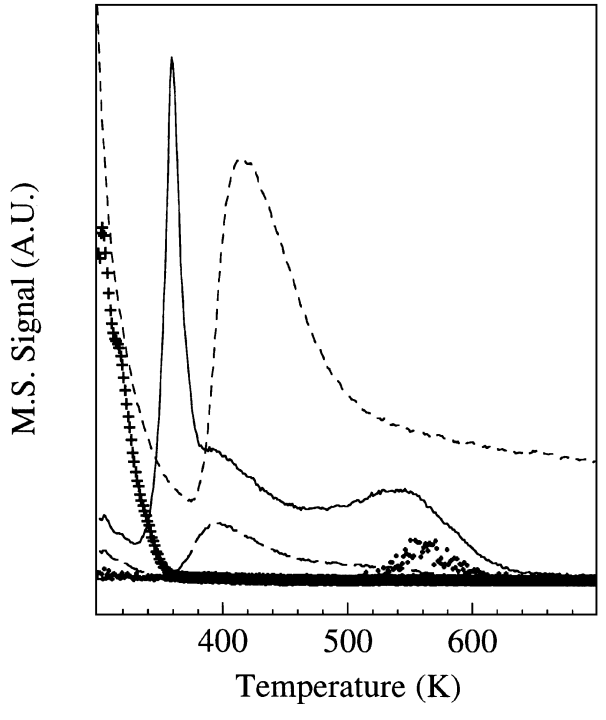

FIG. 9. TPReac of 2-propanol over H-mordenite. $m/e = 41$ (solid), 18 (short-dashed), 45 (+), 58 (long-dashed), and 65 (×10, dotted).

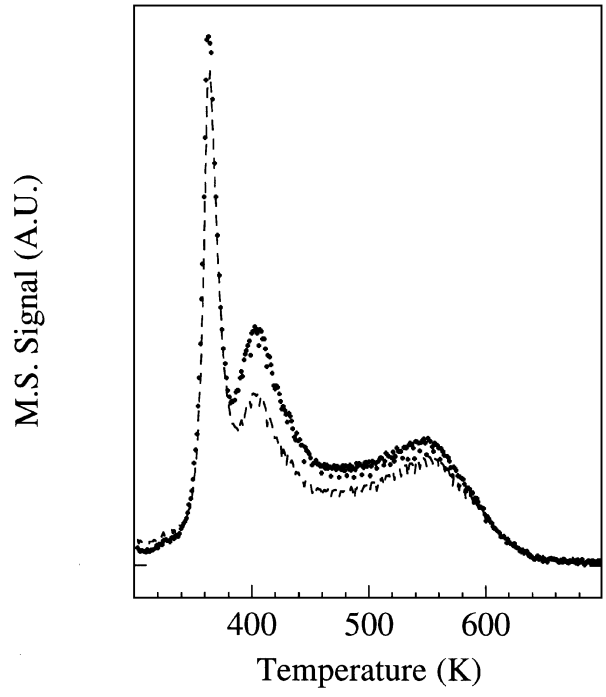

FIG. 10. TPReac of CH_3–HCOD–CH_3 over H-mordenite. $m/e = 41$ (dashed) and 42 (dotted).

an important process over H-mordenite. The reason why a pool of deuterated acid sites is expected to be present long before the onset of reaction is that the energy barrier for H/D exchange between the alcohol and the Brønsted acid sites in the zeolite is known to be very small (18). Readsorption onto Z–OD sites (Z = zeolite lattice) causes deuteration of the hydrocarbon chains. The normal $m/e = 41$ to 42 ratio in unlabeled 2-propanol was approximately 3 : 2 with our mass spectrometer settings. In Fig. 11, it is seen that the extent of exchange is almost negligible in WZ because the 41/42 ratio is essentially that found in unlabeled 2-propanol. We expect the alcohol molecule to chemisorb on WZ much like in the case of alcohol adsorption on molybdena surfaces (19), i.e., by completing the unsaturated coordination sphere of surface M^{6+} adsorption sites via bonding through the alcohol oxygen atom. In this way, and unlike Brønsted (zeolitic) solid acids, the alcohol molecule would not find a vicinal –OH group and be able to undergo H/D exchange prior to reaction (see Fig. 12). The $m/e = 43$ signal in Fig. 11 is not necessarily representative of doubly deuterated species. Rather, it should be taken as indicative of formation of trace amounts of acetone [this is the fragment with the largest intensity in the acetone fragmentation pattern (16, 17)].

Before discussing the possible alcohol dehydration mechanisms occurring on WZ, it is appropriate to briefly mention how alcohol dehydration takes place over acidic zeolites since the two types of catalysts are expected to differ in their behavior significantly. It is now believed that hydrogen

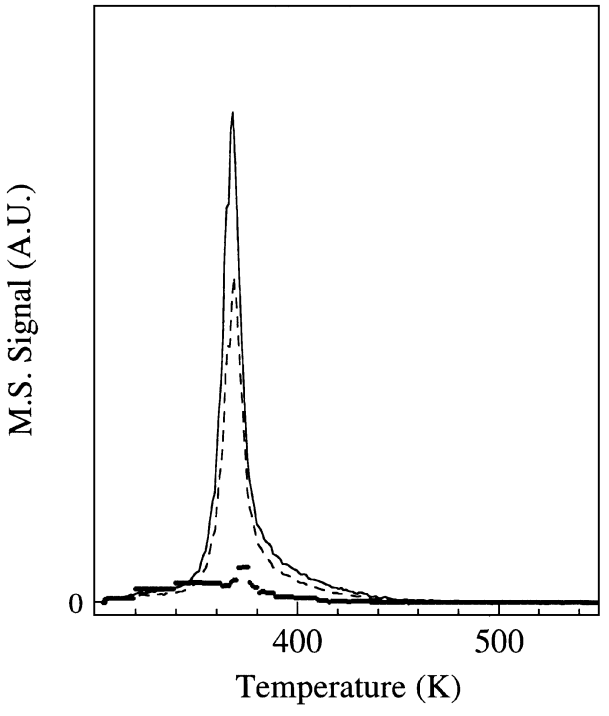

FIG. 11. TPReac of CH_3–HCOD–CH_3 over WZ. $m/e = 41$ (solid), 42 (dashed), and 43 (dotted).

bonding (rather than full protonation) is the preferred adsorption mode of alcohols in zeolites (18). In addition, alcohols have a tendency to displace olefins from the Brønsted acid sites in zeolites (20), and tend to cluster around the acid site by hydrogen bridging (20, 21). Such clustering of two or more alcohol molecules is responsible for negative reaction orders in chemical processes that involve alcohols over zeolitic catalysts (20), and could provide an alterative explanation for the so-called "stop effect," i.e., an increase in reaction rate when the alcohol flow is interrupted (22). Figure 12 indicates that the alcohol dehydration mechanism over H-mordenite and WZ is expected to be different right from the start of the reaction sequence. A metal oxide adsorption site effectively acts as an acid–basic site pair. We have mentioned that alcohols tend to complete the oxygen coordination sphere of unsaturated molybdena moieties [see the interesting EPR work by M. Che *et al*. reviewed in Ref. (19)]. By means of *in situ* infrared spectroscopy, Hussein *et al*. (13) have shown that isopropoxide species are adsorbed on the surface of dehydroxylated HfO_2, TiO_2, and ZrO_2. Other groups have also proposed the presence of alkoxy species adsorbed on chemisorption and/or reaction of 2-propanol over silica–magnesia mixed oxides (23–25). While it is conceivable that the alcohol molecule adsorbs onto the metal oxide center by hydrogen bonding first, we favor the idea that the oxygen from the alcohol hydroxyl group interacts with the metal ion, just as proposed previously by other authors (23–25).

Our proposed reaction scheme for alcohol dehydration over WZ is presented in Fig. 13. Since the disappearance of isopropoxide IR bands correlated well with the appearance of products in the gas phase for a number of metal oxides (13), reaction steps 1 and 2 are not likely to merge into a single, concerted step. On the other hand, it is possible that the alcohol interacts with the oxide surface on

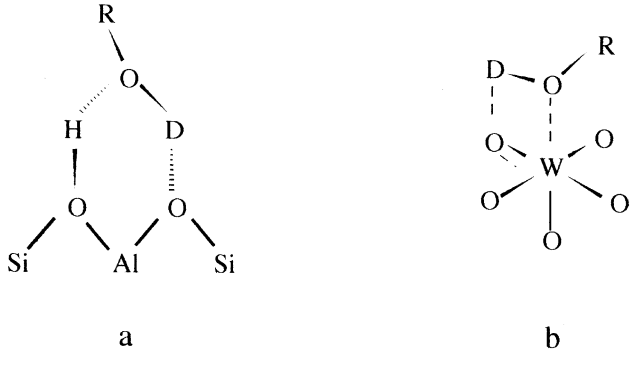

FIG. 12. Alcohol adsorption on (a) zeolite acid sites and (b) metal oxides.

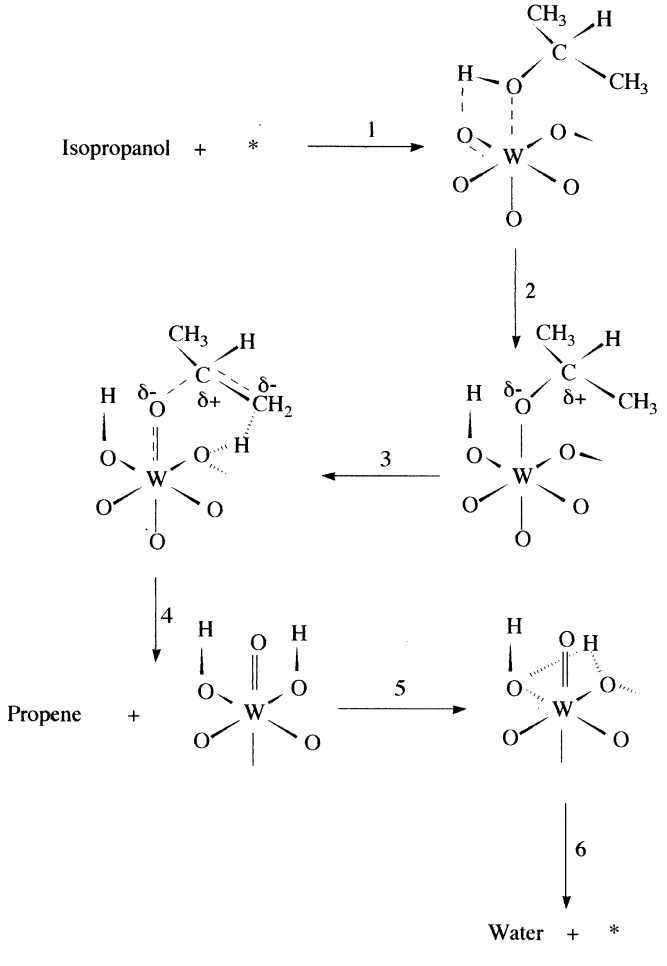

FIG. 13. Proposed reaction scheme.

adsorption before forming the intermediate from step 1; i.e., step 1 may be viewed as the result of alcohol adsorption and subsequent rearrangement. The question that immediately comes to mind is why we chose to propose the involvement of a bridging M–O–M bond at the surface. First, we do not believe that an isolated WO_x moiety is responsible for all the catalysis. These materials achieved their best activity for acid-catalyzed reactions after W–O–W bonds are formed (8). Second, it is also possible that Zr–O–W bonds are involved instead since otherwise WZ would not behave dramatically different than WO_3/Al_2O_3, a fact that is not true for alcohol dehydrations (5). We have considered other possibilities like hydrating the W=O double bond. The resulting *gem*-hydroxyl configuration around W on propene formation (and prior to dehydration) would result in some oxygen exchange between the catalyst and the alcohol. To test this, we exchanged the catalyst by repeated injections of $H_2\ ^{18}O$ at 823 K under He. The exchange was confirmed by following the evolution and the consumption of unlabeled and labeled water, respectively. When the labeled catalyst was used for isopropanol dehydration, we found no evidence for desorption of oxygen-labeled alcohol or oxygen-labeled water of reaction. This suggests that the oxygen in the alcohol molecule is transformed into product water without exchanging with the support under the conditions employed in our work. Note that step 2 would produce a W–OH group from the alcohol oxygen, which could preferentially leave the surface providing both M–OH bonds produced are nonequivalent. We favored the proposal of a six-membered ring intermediate involving the W center over four-membered species because the former should be less subjected to steric hindrance. For example, we could have proposed a structure in which the alkyl hydrogen atom forms a bond with the oxygen atom from the alcohol (a four-membered ring structure).

To be able to observe H^+/D^+ exchange in the product olefin, step 2 must be reversible. Once the hydrated site is formed, it appears that water remains on the surface for approximately 1 more minute after the olefin is formed (see Fig. 8). Such differences between desorption peaks within the same runs are not due to experimental errors. The difference between the olefin and water desorption peaks is even more pronounced in the *tert*.-butanol experiments (Fig. 3). If we assume that adsorption of reactants (which was clearly eliminated by our temperature-programmed techniques) is not rate limiting, water desorption (regeneration of the site) is likely to be the rate-determining step. Clearly, the olefin and water molecules do not leave the adsorption site at the same time, and readsorption of the olefin onto hydrated sites does not seem to take place judging from the lack of H^+/D^+ isotopic exchange of the product olefins over WZ. We must, however, mention that WZ does not behave the same way with deuterated tertiary alcohols; i.e., deuterium is indeed incorporated into the product olefins with tertiary carbon atoms (26). This may be due to some extent to the reversibility in step 2 when using tertiary alcohols instead of 2-propanol. With respect to H-mordenite, readsorption of the olefin onto the acid sites seemed to have occurred. The $m/e = 42$ and 41 signals overlap exactly in the time scale for the H-mordenite sample, suggesting that incorporation of deuterium by readsorption of the alkene is a fast process in zeolites (Fig. 10).

The zirconia support with no oxoanion promoters is expected to largely favor the production of acetone from 2-propanol by dehydrogenation. Using 2-propanol as the test molecule, Hussein *et al*. (13) showed that ZrO_2 dehydroxylated by calcination at 773 K has a higher selectivity toward dehydrogenation to acetone up to 573 K. If the dehydrogenation pathway requires the presence of basic sites and the dehydration reaction makes use of an acid–base pair as recently proposed by Poeppelmeier and co-workers (12), it is apparent that a small population of basic centers is also present in WZ (see Fig. 11).

In summary, a negligible tendency to form alkene oligomers and the existence of (to a small extent) acid–basic site pairs on WZ are some of the key differences between these materials and acidic zeolites. Despite the fact that acidity in WZ calcined at high temperatures is nonprotic in nature, the reactivity of WZ toward 2- and 1-propanol dehydration is comparable to that of H-mordenite. The very low tendency to yield coke by oligomerization of the olefinic products could make WZ a particularly attractive material for acid-catalyzed reactions involving olefins as reactants.

ACKNOWLEDGMENTS

This research was supported by the donors of the Petroleum Research Fund (Grant 31067-AC5). Beamtime at the Brookhaven National Laboratory is gratefully acknowledged. One of us (L.M.P.) thanks the University of San Juan, Argentina, for supporting her graduate work at the University of Nebraska–Lincoln. We thank the referees for their valuable comments.

REFERENCES

1. Hino, M., and Arata, K., *J. Chem. Soc. Chem. Commun.*, 1259 (1987).
2. Iglesia, E., Barton, D. G., Soled, S. L., Miseo, S., Baumgartner, J. E., Gates, W. E., Fuentes, G. A., and Meitzner, G. D., *in* "Proceedings, 11th International Congress on Catalysis" (J. W. Hightower and W. N. Delgass, Eds.), p. 533. Elsevier, Amsterdam, 1996.
3. Larsen, G., Lotero, E., and Parra, R. D., *in* "Proceedings, 11th International Congress on Catalysis" (J. W. Hightower and W. N. Delgass, Eds.), p. 543. Elsevier, Amsterdam, 1996.
4. Larsen, G., Lotero, E., Raghavan, S., Parra, R. D., and Querini, C. A., *Appl. Catal. A* **139**, 201 (1996).
5. Larsen, G., Raghavan, S., Márquez, M., and Lotero, E., *Catal. Lett.* **37**, 57 (1996).
6. Larsen, G., and Petkovic, L. M., *J. Mol. Catal.*, in press.
7. Larsen, G., and Petkovic, L. M., *Appl. Catal. A*, in press.
8. Wachs, I. E., Kim, D. S., and Ostromecki, M., *J. Mol. Catal. A* **106**, 93 (1996).
9. Larsen, G., Lotero, E., Nabity, M., Petkovic, L. M., and Shobe, D. S., *J. Catal.*, in press.

10. Stern, E. A., Newville, M., Ravel, B., Yacoby, Y., and Haskel, D., *Physica B* **208**, 117 (1995).
11. Aronson, M. T., Gorte, R. J., and Farneth, W. E., *J. Catal.* **98**, 434 (1986).
12. Tomczak, D. C., Allen, J. L., and Poeppelmeier, K. R., *J. Catal.* **146**, 155 (1994).
13. Hussein, G. A. M., Sheppard, N., Zaki, M. I., and Fahim, R. B., *J. Chem. Soc. Faraday Trans. 1* **85**, 1723 (1989).
14. Yue, P. L., and Olaofe, O., *Chem. Eng. Res. Dev.* **62**, 81 (1984).
15. Adeeva, V., de Haan, J. W., Jänchen, J., Lei, G. D., Schünemann, V., van de Ven, L. J. M., Sachtler, W. M. H., and van Santen, R. A., *J. Catal.* **151**, 364 (1995).
16. Hall, K. R., *et al.* (Eds.), "TRC Spectral Data—Mass," Vol. 1. Thermodynamics Research Center, Texas A&M Univ., College Station, 1963.
17. Cornu, A., and Massot, R., "Compilation of Mass Spectral Data," Vol. 1, 2nd ed. Heyden, London, 1975.
18. Haase, F., and Sauer, J., *J. Am. Chem. Soc.* **117**, 3780 (1995).
19. Sojka, Z., *Catal. Rev. Sci. Eng.* **37**, 461 (1995).
20. Larsen, G., Lotero, E., Márquez, M., and Silva, H. S., *J. Catal.* **157**, 645 (1995).
21. Mirth, G., Lercher, J. A., Anderson, M. W., and Klinowsky, J., *J. Chem. Soc. Faraday Trans.* **86**, 3039 (1990).
22. Makarova, M. A., Williams, C., Zamaraev, K. I., and Thomas, J. M., *J. Chem. Soc. Faraday Trans.* **90**, 2147 (1994).
23. Miyata, H., Wakamiya, M., and Kubokawa, Y., *J. Catal.* **34**, 117 (1974).
24. Takezawa, N., Hanamaki, C., and Kobayashi, H., *J. Catal.* **38**, 101 (1975).
25. Noller, H., and Ritter, G., *J. Chem. Soc. Faraday Trans. 1* **80**, 275 (1984).
26. Larsen, G., Lotero, E., Nabity, M., Petkovic, L. M., and Querini, C. A., *in* "Proceedings, 5th International Symposium on Catalyst Deactivation, Mexico, 1997," in press.